

## Accepted Manuscript

Synthesis of platinum(II) Complexes of Isatin Thiosemicarbazones Derivatives:  
*In Vitro* Anti-cancer and Deoxyribosenucleic Acid Binding Activities

Amna Qasem Ali, Siang Guan Teoh, Abdussalam Salhin, Naser Eltaher Eltayeb,  
Mohamed B. Khadeer Ahamed, A.M.S. Abdul Majid

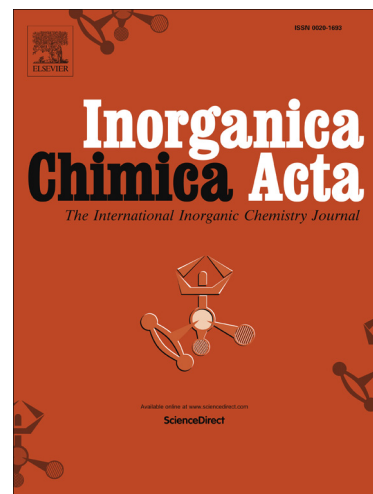
PII: S0020-1693(14)00183-2  
DOI: <http://dx.doi.org/10.1016/j.ica.2014.03.029>  
Reference: ICA 15929

To appear in: *Inorganica Chimica Acta*

Received Date: 14 November 2013  
Revised Date: 19 February 2014  
Accepted Date: 16 March 2014

Please cite this article as: A.Q. Ali, S.G. Teoh, A. Salhin, N.E. Eltayeb, M.B. Khadeer Ahamed, A.M.S. Abdul Majid, Synthesis of platinum(II) Complexes of Isatin Thiosemicarbazones Derivatives: *In Vitro* Anti-cancer and Deoxyribosenucleic Acid Binding Activities, *Inorganica Chimica Acta* (2014), doi: <http://dx.doi.org/10.1016/j.ica.2014.03.029>

This is a PDF file of an unedited manuscript that has been accepted for publication. As a service to our customers we are providing this early version of the manuscript. The manuscript will undergo copyediting, typesetting, and review of the resulting proof before it is published in its final form. Please note that during the production process errors may be discovered which could affect the content, and all legal disclaimers that apply to the journal pertain.



**Synthesis of platinum(II) Complexes of Isatin Thiosemicarbazones Derivatives : *In Vitro*****Anti-cancer and Deoxyribonucleic Acid Binding Activities****Amna Qasem Ali <sup>a</sup>, Siang Guan Teoh <sup>a\*</sup>, Abdussalam Salhin <sup>a</sup>, Naser Eltahir Eltayeb <sup>b</sup>,****Mohamed B. Khadeer Ahamed <sup>c</sup> and AMS Abdul Majid <sup>c</sup>**

<sup>a</sup>School of Chemical Sciences, Universiti Sains Malaysia, Minden-11800, Pulau Pinang,  
Malaysia,

<sup>b</sup>Department of Chemistry, Sciences & Arts College – Rabigh, King AbdullAziz University ,  
Rabigh , Saudi Arabia,

<sup>c</sup>EMAN Research and Testing Laboratory, School of Pharmaceutical Sciences,  
Universiti Sains Malaysia, 11800-Minden, Pulau Pinang, Malaysia

**Corresponding Author:**

\* **Corresponding Author:** Prof. Dr. Siang Guan Teoh

**Corresponding Address:**

School of Chemical Sciences,  
Universiti Sains Malaysia,  
Minden, Pinang, Malaysia,  
Email : [sgteoh@usm.my](mailto:sgteoh@usm.my)  
Tel : (604)-6577888 ext 3565  
Fax: (604)-6574854

**Abstract**

Six new platinum(II) complexes of a thiosemicarbazone Schiff base with isatin moiety [PtL1 to Pt(L6)<sub>2</sub>] were synthesized by the reaction of platinum(II) with the following: (Z)-2-(2-oxoindolin-3-ylidene)-N-phenylhydrazinecarbothioamide [L1H], (Z)-2-(5-methyl-2-oxoindolin-3-ylidene)-N-phenylhydrazinecarbothioamide [L2H], (Z)-2-(5-fluoro-2-oxoindolin-3-ylidene)-N-phenylhydrazinecarbothioamide [L3H], (Z)-N-methyl-2-(5-nitro-2-oxoindolin-3-ylidene)hydrazinecarbothioamide [L4H], (Z)-N-methyl-2-(5-methyl-2-oxoindolin-3-ylidene)hydrazinecarbothioamide [L5H], and (Z)-N-ethyl-2-(5-methyl-2-oxoindolin-3-ylidene)hydrazinecarbothioamide [L6H]. The structures of these complexes were characterized by elemental analysis, IR, UV-vis, <sup>1</sup>H NMR, and mass spectrometry analyses. The structure of Pt(L6)<sub>2</sub> was further characterized by single-crystal XRD. The interaction of these complexes with calf thymus (CT) DNA exhibited a high intrinsic binding constant ( $K_b = 3.5 \times 10^4$  to  $3.29 \times 10^6 \text{ M}^{-1}$ ), which reflected the intercalative activity of these complexes toward CT DNA. This result was also confirmed by viscosity data. Data obtained from the *in vitro* anti-proliferative study clearly established the anticancer potency of PtL1, PtL2, PtL3, PtL5, and Pt(L6)<sub>2</sub> against the human colorectal carcinoma cell line HCT 116.

Keywords: Platinum(II) complexes, isatin moiety, intercalative activity, anti-proliferative study

**1. Introduction**

Cisplatin (cis-diamminedichloroplatinum(II) or cis-[PtCl<sub>2</sub>(NH<sub>3</sub>)<sub>2</sub>]) is one of the most potent antitumor drugs available for the therapeutic management of solid tumors, such as germ cell tumors, ovarian, lung, head and neck, and bladder cancers. Cisplatin promotes cancer cell death by binding to DNA [1-3]. However, cisplatin has the shortcomings of nephrotoxicity, low

water solubility, and intrinsic resistance that limit its clinical application [4-7]. One of the mechanisms inducing nephrotoxicity is the inactivation of some enzymes caused by the reaction between platinum ions and sulfur-containing proteins. Hence, the synthesis of new types of compounds whose structure and mode of action differ from those of cisplatin and bearing nitrogen and sulfur mixed donor atoms is important to prevent adverse reactions. Anticancer drugs that target DNA have two different interaction mechanisms, namely, covalent binding or noncovalent interactions. Cisplatin is known to bind to DNA through covalent bonding through chloride ligand exchange with a nitrogen base of DNA. Non-covalent interactions between DNA and anticancer drugs are classified into three, i.e., electrostatic interactions with the negatively charged phosphate backbone of DNA, binding interactions to the minor and major grooves of DNA double helix, and intercalation of a planar aromatic ligand between two base pairs through  $\pi$ -stacking [8]. One of most typical tridentate NNS chelate ligands is *a*-(*N*)-heterocyclic thiosemicarbazones. Several mechanisms of antitumor action have been proposed for this class of chelate ligands and their complexes. They could interact with DNA by formation of a metal-DNA covalent bond, by interfering in DNA synthesis by ribonucleotide reductase inhibition, or by interacting with DNA through non-covalent interactions including H-bonding and intercalation [9]. Intercalation and groove binding are the most important DNA-binding modes because they invariably lead to cellular degradation [10]. The current work describes the *in vitro* anticancer activity of Pt(II) complexes of thiosemicarbazones of the combinatorial mixtures of isatin derivatives. DNA binding of these complexes were conducted to evaluate the DNA binding modes. The synthesis, physicochemical characterization and DNA binding activity of mono platinum(II) complexes with bidentate ligands were reported. The *in vitro* cytotoxic activities of compounds were tested against the human colorectal carcinoma cell line HCT 116.

## 2. Experimental

### 2.1. Materials and methods

Isatin, 5-fluoroisatin, 5-methylisatin, 5-nitroisatin, 4-ethyl-3-thiosemicarbazide, 4-methyl-3-thiosemicarbazide, 4-phenyl-3-thiosemicarbazide, and potassium tetrachloroplatinate(II) were purchased from Aldrich Chemicals. 3-(4, 5-Dimethylthiazol-2-yl)-2,5-diphenyl tetrazolium bromide (MTT) was purchased from Sigma–Aldrich, Germany. Commercial-grade solvents and reagents were used as supplied without further purification. Calf thymus (CT) DNA, agarose (molecular biology grade), and ethidium bromide (EB) were from Sigma (St. Louis, MO, USA). Elemental analysis was carried out using a PerkinElmer 2400 series-11 CHN/O analyzer (Waltham, MA, USA). Infrared, electronic, nuclear magnetic resonance, and fluorescent spectra were recorded on PerkinElmer 2000, Perkin Elmer-Lambda 25, and Bruker 500 MHz spectrometer at room temperature using DMSO-d<sub>6</sub> using as solvent and TMS as an internal standard. and Jasco FP-750 spectrophotometers, respectively. Viscosity measurements were made using a Cannon Manning Semi-Micro viscometer (State College, PA, USA). ESI-mass spectra were obtained using Liquid Chromatography/Mass Spectrometry LC/MSD Trap VL (Agilent Technologies), it was operated in either positive ion or negative ion detection mode.

### 2.2. Synthesis of ligands

Schiff bases (L1H to L6H) have been recently synthesized and characterized in our laboratory [11-15]. In brief, Schiff base ligands were synthesized by refluxing the reaction mixture of hot ethanolic solutions (30 ml each) of 4-substituted-3-thiosemicarbazide (0.01 mol) and 5-substituted isatin (0.01 mol) for 2 h. The precipitates that formed during reflux were filtered and washed with cold ethanol (Scheme 1).

[Insert Scheme 1]

### 2.3. Synthesis of complexes

The Pt(II) complexes were synthesized by refluxing the reaction mixture of hot ethanolic solutions (30 ml each) of  $K_2PtCl_4$  (0.01 mol) and appropriate ligand (0.01 mol) for 2 h. The precipitates that formed during reflux were filtered and washed with cold ethanol (Scheme 2).

[Insert Scheme 2]

**2.3.1.  $C_{15}H_{11}ClN_4OPtS$  (PtL1):** Black; MP:  $>300$  °C; yield: 72%; analytical calculated values C (34.26%); H (2.11%); N (10.65%); Pt (37.10%); analytical results (experimental): C (34.45%); H (2.42%); N (10.51%); Pt (37.22%); selected IR data (KBr pellet,  $\nu_{max}/cm^{-1}$ ): 3309–3143 (NH), 1637 (C=O), 1614 (C=N), 767 (C-S);  $^1H$  NMR (500 MHz, DMSO- $d_6$ ) ( $\delta$  (ppm)): 11.09 (s, 1 H, indole N-H), 10.62 (s, 1 H, CS-NH), 8.13 (d, 1 H, indole C2-H,  $J = 5.3$  Hz), 7.50 (d, 2 H, thiosemicarbazide C11-H, C15-H,  $J = 7.4$  Hz), 7.45 to 7.41 (t, 2 H, thiosemicarbazide C12-H, C14-H,  $J = 7.8$ ), 7.40 to 7.38 (dd, 1 H, indole C3-H,  $J = 7.7, 1.1$  Hz), 7.21 to 7.19 (t, 1 H, thiosemicarbazide C13-H,  $J = 7.3$ ), 6.90 to 6.85 (q, 2 H, indole C4-H, C5,  $J = 7.6$  Hz); UV-vis [DMSO  $\lambda_{max}$ , nm]: 264, 409, 446 and ESI-MS ( $m/z$ ): 523 (M-2H) $^{2-}$ .

**2.3.2.  $C_{16}H_{13}ClN_4OPtS$  (PtL2):** Black; MP:  $>300$  °C; yield: 78%; analytical calculated values: C (35.59%); H (2.43%); N (10.38%); Pt (36.13%); analytical results (experimental): C (35.60%); H (2.17%); N (10.16%); Pt (36.20%); selected IR data (KBr pellet,  $\nu_{max}/cm^{-1}$ ): 3326 to 3136 (NH), 1636 (C=O), 1613 (C=N), 750 (C-S);  $^1H$  NMR (500 MHz, DMSO- $d_6$ ) ( $\delta$  (ppm)): 11.95 (s, 1 H, indole N-H), 10.56 (s, 1 H, CS-NH), 7.94 (s, 1 H,

indole C5-H), 7.51 (d, 2H, thiosemicarbazide C11-H, C15-H,  $J = 7.7$  Hz), 7.45 to 7.42 (t, 2 H, thiosemicarbazide C12-H, C14-H,  $J = 7.8$  Hz), 7.22 to 7.19 (t, 2 H, indole C3-H, thiosemicarbazide C13-H,  $J = 7.1$  Hz), 6.74 (d, 1 H, indole C2-H,  $J = 7.9$ ), 2.13 (s, 3 H, CH<sub>3</sub>); UV-vis [DMSO  $\lambda_{\max}$ , nm]: 265, 409, 450 and ESI-MS ( $m/z$ ): 537.8 (M-2H)<sup>2-</sup>.

**2.3.3. C<sub>15</sub>H<sub>10</sub>ClFN<sub>4</sub>OPtS (PtL3):** Brown; MP: >300 °C; yield: 72%; analytical calculated values C (33.13%); H (1.85%); N (10.30%); Pt (35.87%); analytical results (experimental): C (33.25%); H (1.63%); N (10.56%); Pt (14.20%); selected IR data (KBr pellet,  $\nu_{\max}/\text{cm}^{-1}$ ): 3308 (NH), 1637 (C=O), 1618 (C=N), 774 (C-S); <sup>1</sup>H NMR (500 MHz, DMSO-d<sub>6</sub>) ( $\delta$  (ppm)): 11.08 (s, 1 H, indole N-H), 10.79 (s, 1 H, CS-NH), 7.91 (s, 1 H, indole C5-H), 7.48 (d, 2 H, thiosemicarbazide C11-H, C15-H,  $J = 7.7$  Hz), 7.44 to 7.14 (t, 2 H, thiosemicarbazide C12-H, C14-H,  $J = 7.7$  Hz), 7.28 to 7.21 (m, 2 H, indole C3-H, thiosemicarbazide C13-H), 6.86 to 6.83 (dd, 1 H, indole C2-H,  $J = 8.5, 4.3$  Hz); UV-vis [DMSO  $\lambda_{\max}$ , nm]: 265, 406, 452 and ESI-MS ( $m/z$ ): 540.7 (M-2H)<sup>2-</sup>.

**2.3.4. C<sub>10</sub>H<sub>8</sub>ClN<sub>5</sub>O<sub>3</sub>PtS (PtL4):** Dark brown; MP: >300 °C; yield: 78%. analytical calculated values C (23.61%); H (1.58%); N (13.76%); Pt (38.34%); analytical results (experimental): C (23.58%); H (1.49%); N (13.44%); Pt (38.17%); selected IR data (KBr pellet,  $\nu_{\max}/\text{cm}^{-1}$ ): 3155 (NH), 1640 (C=O), 1625 (C=N), 741 (C-S); <sup>1</sup>H NMR (500 MHz, DMSO-d<sub>6</sub>) ( $\delta$  (ppm)): 11.83 (s, 1 H, indole N-H), 9.56 to 9.54 (q, 1 H, CS-NH,  $J = 8.8, 4.3$  Hz), 8.53 (d, 1 H, indole C5-H,  $J = 2.3$  Hz), 8.28 to 8.26 (dd, 1 H, indole C3-H,  $J = 6.3, 2.4$  Hz), 7.13 (d, 1 H, indole C2-H,  $J = 8.7$  Hz), 3.10 (d, 3H, thiosemicarbazide CH<sub>3</sub>,  $J = 4.5$  Hz); UV-vis [DMSO  $\lambda_{\max}$ , nm]: 259, 395, 450 and ESI-MS ( $m/z$ ): 508.8 (M+H)<sup>+</sup>.

**2.3.5. C<sub>11</sub>H<sub>11</sub>CIN<sub>4</sub>OPtS (PtL5):** Dark brown; MP: >300 °C; yield: 81%; analytical calculated values C (27.65%); H (2.32%); N (11.73%); Pt (40.83%); analytical results (experimental): C (27.95%); H (2.31%); N (11.84%); Pt (40.62%); selected IR data (KBr pellet,  $\nu_{\max}/\text{cm}^{-1}$ ): 3278 (NH), 1658 (C=O), 1615 (C=N), 765 (C-S); <sup>1</sup>H NMR (500 MHz, DMSO-d<sub>6</sub>) ( $\delta$  (ppm)): 11.25 (s, 1 H, indole N-H), 9.25 to 9.23 (q, 1 H, CS-NH), 7.95 to 7.47 (dd, 1 H, indole C5-H), 7.25 to 7.16 (m, 1 H, indole C3-H), 6.89 to 7.77 (ddd, 1 H, indole C2-H, J = 7.9 Hz), 3.10 (dd, 3 H, thiosemicarbazide CH<sub>3</sub>, J = 4.6 Hz), 2.27 (s, 3 H, indole CH<sub>3</sub>); UV-vis [DMSO  $\lambda_{\max}$ , nm]: 265, 390, 460 and ESI-MS ( $m/z$ ): 474.8 (M-2H)<sup>2+</sup>.

**2.3.6. C<sub>24</sub>H<sub>26</sub>N<sub>8</sub>O<sub>2</sub>PtS<sub>2</sub> (Pt(L6)<sub>2</sub>):** The characterization data correspond to powder. Brown; MP: >300 °C; yield: 75%; analytical calculated values C (40.16%); H (3.65%); N (15.61%); Pt (27.78%); analytical results (experimental): C (40.21%); H (3.46%); N (15.39%); Pt (27.57%); selected IR data (KBr pellet,  $\nu_{\max}/\text{cm}^{-1}$ ): 3223 to 3180 (NH), 1693 (C=O), 1618 (C=N), 788 (C-S); <sup>1</sup>H NMR (500 MHz, DMSO-d<sub>6</sub>) ( $\delta$  (ppm)): 11.11 (s, 1H, indole N-H), 9.29 to 9.27 (t, 1H, CS-NH, J = 5.6 Hz), 7.50 (s, 1 H, indole C5-H), 7.18 to 7.16 (dd, 1 H, indole C2-H, J = 7.9 Hz), 6.83 to 6.76 (dd, 1 H, indole C3-H, J = 7.9 Hz), 3.66 to 3.61 (p, 2 H, thiosemicarbazide CH<sub>2</sub>, J = 6.6 Hz), 2.30 (s, 3H, indole CH<sub>3</sub>), 1.24 to 1.20 (t, 3H, thiosemicarbazide CH<sub>3</sub>, J = 7.1); and UV-vis [DMSO  $\lambda_{\max}$ , nm]: 266, 389, 455.

## 2.4. X-ray crystallography

Single crystals of compound **Pt(L6)<sub>2</sub>** suitable for diffraction were grown by slow evaporation of 3:1 mixtures of acetone and DMF. Selected crystal data and data collection parameters are presented in Table 1. Data of Pt(L6)<sub>2</sub> were collected on a Bruker SMART APEX II CCD diffractometer [16] equipped with graphite monochromatized Mo K $\alpha$  radiation ( $\lambda = 0.71073$  ) at 100(1) K. Multi-scan absorption corrections were applied using the

SADABS program [16]. The structure was solved by the direct method using the SHELXS-97 program [17]. Refinements on F2 were performed using SHELXL-97 by the full-matrix least-square method with anisotropic thermal parameters for all non-hydrogen atoms. N-bound H atoms were located in a difference Fourier map and were freely refined. The remaining H atoms were geometrically positioned and refined using a riding model. The program SHELXTL [17] was used to prepare Figs. 1 and 2.

**[Insert Table1]**

### **2.5. DNA interaction studies**

DNA binding experiments including absorption, emission spectral studies, and viscosity measurements conformed to the standard methods [18- 20]. Concentrated CT DNA stock solution was prepared in 5 mM Tris– HCl/50 mM NaCl in water at pH=7.2. The DNA concentration per nucleotide was determined by absorption spectroscopy using the molar absorption coefficient ( $6600 \text{ M}^{-1} \text{ cm}^{-1}$ ) at 260 nm [21]. The purity of the CT DNA was verified by taking the ratio of the absorbance values at 260 and 280 nm in the respective buffer, which was found to be >1.9, indicating that, the DNA was sufficiently free of protein. The stock solutions were stored at 4 °C and used within 4 days. The DNA binding experiments were performed at room temperature. All experiments were carried out by keeping the concentration of platinum complexes constant (50  $\mu\text{M}$ ) while varying the DNA concentration (0 to 200  $\mu\text{M}$ ). An equal amount of DNA was added to the platinum complexes cuvette and the reference cuvette to eliminate the absorbance of CT DNA itself [22, 23], and Tris buffer was subtracted through baseline correction. The UV–Vis and the emission spectra were recorded after equilibration for 10 min after each addition. Viscosity experiments were

carried out using a Cannon Manning Semi-Micro viscometer (State College, PA, USA) thermostated in a water bath maintained at  $37.0 \pm 0.1$  °C. The flow rates of Tris–HCl buffer (pH 7.2), DNA (200  $\mu$ M), and DNA in the presence of Pt(II) complexes at various concentrations ( $0$ – $2.5 \times 10^{-4}$ M) were measured three times each with a digital stopwatch, and the average flow time was calculated. Data were presented as  $(\eta/\eta_0)^{1/3}$  versus the ratio of the concentration of the compound to CT DNA, where  $\eta$  is the viscosity of DNA in the presence of complex, and  $\eta_0$  is that of DNA alone. Viscosity values were calculated from the observed flow time of DNA containing solutions ( $t$ ) corrected for that buffer alone (Tris–HCl/NaCl, 5:50 mM) ( $t_0$ ), and  $\eta = (t - t_0)$ .

## 2.6. Anti-proliferative activity

### 2.6.1. Preparation of cell culture

HCT 116 cells were allowed to grow under optimal incubator conditions. Cells that had reached a confluence of 70%–80% were chosen for cell plating. Old medium was aspirated out of the plate, and then cells were washed using sterile phosphate buffered saline (PBS; pH 7.4) two to three times. PBS was completely discarded after washing. Trypsin was added and evenly distributed onto the cell surface, and the cells were incubated at 37 °C in 5% CO<sub>2</sub> for 1 min. Afterwards, the flasks containing the cells were gently tapped to aid cell segregation and observed under an inverted microscope (if cell segregation was not satisfactory, the cells were incubated for another minute). Trypsin activity was inhibited by adding 5 ml of fresh complete medium (10% FBS). Cells were counted and diluted to get a final concentration of  $2.5 \times 10^5$  cells/ml, and seeded into wells (100  $\mu$ L cells/well). Finally, the cell-containing plates were incubated at 37 °C with an internal atmosphere of 5% CO<sub>2</sub>.

### 2.6.2. MTT assay

Cancer cells (100  $\mu$ l cells/well,  $1.5 \times 10^5$  cells/ml) were seeded on a 96-well microtitre plate, which was incubated with CO<sub>2</sub> overnight to allow cell attachment. The compounds were diluted with media into the required concentrations from the stock. Various concentrations (6.25–200  $\mu$ M) of 100  $\mu$ l of test substances were separately added to each well containing the cells. Then, the plates were incubated at 37 °C with an internal atmosphere of 5% CO<sub>2</sub> incubator for 48 h. After this treatment period, the plates were treated with 20  $\mu$ l of MTT reagent and incubated again for 4 h. After this incubation period, 50  $\mu$ l of MTT lysis solution (DMSO) was added to the wells, and the plates were further incubated for 5 min at room temperature. Finally, the absorbance at 570 and 620 nm wavelengths was measured using a standard Infinite 200 PRO multimode microplate reader (Tecan, USA). Data were recorded and analyzed to estimate the effects of test compounds on cell viability and growth inhibition. The percentage inhibition of cell proliferation was calculated from the optical density obtained from the MTT assay. 5-Fluorouracil (5-FU) was used as the standard reference drug [24]. Statistical difference between the treatments and control were evaluated by one-way ANOVA followed by Tukey's multiple comparison test. Differences were considered significant at  $p < 0.05$  and  $p < 0.01$ .

### **3. Results and discussion**

The platinum(II) complexes PtL1 to Pt(L6)<sub>2</sub> were obtained in good yield from the reaction of potassium tetrachloro platinate(II) with appropriate Schiff base (L1H to L6H) in 1:1 M ratio in the ethanol medium with reflux for 2 h (via Scheme 2). These complexes were insoluble in common organic solvents, but soluble in DMF and DMSO.

#### **3.1. Spectroscopic properties**

##### **3.1.1. IR studies**

The characteristic IR bands recorded for the free ligands differ from those of the related complexes and provided significant indications of the bonding sites of thiosemicarbazone ligands. In comparison with the spectra of the Schiff base, the PtL1 to PtL5 exhibited the band of  $\nu(\text{C}=\text{O})$  within  $1637\text{--}1658\text{ cm}^{-1}$ , showing a shift of the band to lower wavenumbers. This finding indicates that the carbonyl oxygen is coordinated to the metal ion. Meanwhile, the IR spectrum of the  $\text{Pt}(\text{L6})_2$  complex shows the carbonyl oxygen band as a strong band at  $1693\text{ cm}^{-1}$ , suggesting that the  $(\text{C}=\text{O})$  group does not participate in bonding. The band of  $\nu(\text{C}=\text{N})$  within  $1613\text{--}1625\text{ cm}^{-1}$  in the metal complexes shows a shift of the band to lower wavenumbers, which indicates that the nitrogen atom of the azomethine group is coordinated to the metal ion. This finding is further supported by the band at around  $741\text{--}788\text{ cm}^{-1}$  in the metal complexes because of  $\nu(\text{C}-\text{S})$  [25]. Thus, the IR spectral results of PtL1–Pt(L6)<sub>2</sub> provide strong evidence for the complexation of Schiff bases with metal ions in tridentate mode, whereas the ligand L6 coordinates to the platinum ion in a bidentate manner.

### 3.1.2. <sup>1</sup>H NMR

The <sup>1</sup>H NMR (d<sub>6</sub>-DMSO) spectra of Pt(II) complexes show approximately the same peaks identical to those of the free ligands, except that the peak due to the NH group resonance is absent. This finding is considered as additional evidence of the deprotonation of NH.

### 3.1.3. UV-vis Studies

The UV-vis absorption spectra of the Pt(II) complexes were measured within the UV-vis region (200–800 nm) using DMSO. Two absorption bands with varied intensity can be observed. The bands observed within 389–409 nm) are attributable to metal-to-ligand charge

transfer transitions, whereas the bands observed at lower frequencies within 446–455 nm correspond to d–d transitions [26, 27].

### 3.1.4. MS studies

The mass spectra of PtL1, PtL2, PtL3, and PtL5) recorded in the negative mode give peaks at  $m/z$  523, 537.8, 540.7, and 474.8, respectively. This result indicates the presence of complexes  $[M-2H]^{2-}$ ,  $[M-2H]^{2-}$ ,  $[M-2H]^{2-}$ , and  $[M-2H]^{2-}$ , respectively. Meanwhile, the mass spectrum of PtL4 recorded in the positive mode gives a peak at  $m/z$  508.8, indicating the presence of this complex as  $[M+H]^+$ .

### 3.2. Crystal structure of Pt(L6)<sub>2</sub>

The molecular structure of Pt(L6)<sub>2</sub> along with the atom numbering scheme is shown in Fig. 1. Pt(L6)<sub>2</sub> (cis-Pt(C<sub>12</sub>H<sub>13</sub>N<sub>4</sub>O<sub>5</sub>)<sub>2</sub>) presents a square-planar geometry that is slightly distorted around the platinum atom, with the basal plane occupied by the S(1), S(1A), N(2) and N(2A) atoms of two cis-thiosemicarbazone ligands. The distortion is evident from the bond angles S(1)-Pt(1)-N(2) 82.46(7)°, S(1)-Pt(1)-S(1A) 95.71(3)°, S(1)-Pt(1)-N(2A) 174.46(6)°, S(1A)-Pt(1)-N(2) 174.46(6)°, N(2)-Pt(1)-N(2A) 99.84(10)°, and S(1A)-Pt(1)-N(2A) 82.46(7)°, as well as the bond lengths Pt(1)-S(1) 2.2537(8) Å, Pt(1)-N(2) 2.039(3) Å, Pt(1)-S(1A) 2.2537(8) Å, and Pt(1)-N(2A) 2.039(3) Å. Fig. 2 shows the crystal packing of Pt(L6)<sub>2</sub> viewed approximately along the *a*-axis. In the crystal, the molecules are connected together through N-H...O intermolecular interactions into an infinite-one dimensional chain through *c*-axis forming zigzag shape (Fig. 2).

[Insert Fig. 1 and Fig. 2]

### 3.3. DNA interaction studies

#### 3.3.1. Absorption spectrum studies

One of the most useful techniques for studying the DNA binding of molecules is electronic absorption spectroscopy. DNA usually results in hypochromism and red shifting (bathchromism) as a consequence of the intercalation mode involving a strong stacking interaction between an aromatic chromophore and the DNA base pairs [28]. It arises from the contraction of CT DNA in the helix axis and its conformational changes [29, 30]. Meanwhile, hyperchromism results from the secondary distortion of the DNA double-helix structure [31, 32]; the extent of hyperchromism indicates partial or non-intercalative binding modes [33]. The absorption spectra of 50  $\mu\text{M}$  PtL3 and Pt(L6)<sub>2</sub> in the absence and presence of CT DNA (0 to 200  $\mu\text{M}$ ) are given in Figs. 3 and 4; the absorption spectra of PtL1, PtL2, PtL4, and PtL5 are given in the Supplementary material (Figs. S1 –S4). The absorption spectra of PtL1 and Pt(L6)<sub>2</sub> display clear hypochromism with a slight blue shift  $\sim 3\text{--}4$  nm. After the compounds intercalate to the DNA base pairs, the  $\pi^*$  orbital of the intercalate compounds couples with the  $\pi$  orbitals of the base pairs, thereby decreasing the  $\pi \rightarrow \pi^*$  transition energies. These interactions result in the observed hypochromism [34]. The hypochromism of these complexes follows the order of Pt(L6)<sub>2</sub> > PtL1. Remarkably, PtL2, PtL3, PtL4, and PtL5 exhibit both hypochromism and hyperchromism at  $\sim 402 - 444$  and  $\sim 255$  nm, respectively, suggesting that the DNA double-helix structure is distorted after the complex binds to DNA through the intercalation mode [35]. This behavior has been reported for chiral Schiff base complexes [36, 37]. PtL1, PtL2, PtL3 and Pt(L6)<sub>2</sub> show hypochromism with a blue shift of  $\sim 3$  nm, whereas PtL4 and PtL5 display a small blue shift of  $\sim 1$  nm. The intrinsic binding constant of all complexes with DNA was determined by observing the changes in absorbance of the complexes with increased DNA concentration using the following equation [38, 39]:

$$[\text{DNA}]/(\varepsilon_a - \varepsilon_f) = [\text{DNA}]/(\varepsilon_b - \varepsilon_f) + 1/K_b(\varepsilon_b - \varepsilon_f)$$

where  $\varepsilon_a$ ,  $\varepsilon_f$ , and  $\varepsilon_b$  are the extinction coefficients observed for the absorption band at a given DNA concentration for free and bound complex, respectively; [DNA] is the concentration of DNA in base pairs; and the binding constant  $K_b$  was determined from the slope-to-intercept ratio by plotting  $[DNA]/(\varepsilon_a - \varepsilon_f)$  vs. [DNA] (Figs. 3a and 4a). The intrinsic binding constant ( $K_b$ ) for PtL1, PtL2, PtL3, PtL4, PtL5, and Pt(L6)<sub>2</sub> are found to be  $1.59 \times 10^6$ ,  $6.3 \times 10^5$ ,  $3.29 \times 10^6$ ,  $3.5 \times 10^4$ ,  $3.6 \times 10^5$ , and  $8.9 \times 10^5 \text{ M}^{-1}$ , respectively. The DNA binding abilities of PtL1, PtL2 and PtL3 are higher compared to other platinum complexes. This is attributed to the effective stacking interaction in the former due to the presence of an extended aromatic phenyl ring which allows an intercalating ligand deeply into the DNA base pairs. The  $K_p$  for PtL3 is too high maybe due to the presence of fluorine atom at C5 [40]. Comparison of the intrinsic binding constants of these complexes with those of DNA-intercalative Pt(II) complexes such as  $[\text{Pt}(\text{bpy})(\text{pip})]^{2+}$  and  $[\text{Pt}(\text{bpy})(\text{hpip})]^{2+}$  [41] reveals that these complexes bind to DNA by intercalation, but proving the binding mode requires more experiments.

**[Insert Fig. 3 and Fig. 4]**

### 3.3.2. Emission spectrum studies

To further study the interaction mode between PtL1–Pt(L6)<sub>2</sub> and CT DNA, fluorescence titration experiments were performed. These complexes are found to emit luminescence in Tris–HCl/NaCl buffer at room temperature with maximum wavelengths of about 379 nm (Supplementary material, Figs. S5–S8). The emission spectra of PtL2 and Pt(L6)<sub>2</sub> (50  $\mu\text{M}$ ) in the absence and presence of CT DNA (0 to 200  $\mu\text{M}$ ) are shown in Figs. 5 and 6. The emission intensity increases with increased CT DNA concentration. These

observations imply that these complexes can strongly interact with CT DNA and propose an intercalative mode with the base pairs of the DNA helix [42].

[Insert Fig. 5 and Fig. 6]

### 3.3.3. Viscosity measurements

The most critical and least ambiguous tests of a binding in solution in the absence of crystallographic data [43, 44] are hydrodynamic measurements (i.e., viscosity and sedimentation), which are sensitive to length changes. A classical intercalation molecule such as EB lengthens the DNA helix, leading to increased DNA viscosity caused by an increase in the separation of base pairs at the interaction site and an increase in the overall double-helix length. Meanwhile, partial or nonclassical intercalation of the complex results in the bending of the DNA helix that reduces the effective DNA length and viscosities. By contrast, an electrostatic or groove binding mode has minimal effects on DNA viscosities [45, 46]. The viscosity measurements of PtL1 to Pt(L6)<sub>2</sub> and EB are shown in **Figs. 7 and 8**. The plot of relative specific viscosity versus [complex]/[DNA] ratio shows a significant increase in the ratio upon addition of the complex. These observations suggest the intercalative binding of these complexes to the DNA double helix [47, 48], in agreement with the results of optical absorption experiments.

[Insert Fig. 7 and Fig. 8]

### 3.4. Anti-proliferative activity

The *in vitro* anti-proliferative activity of PtL1–Pt(L6)<sub>2</sub> was evaluated against HCT116 cells. **Fig. 9** shows the effect of different concentrations of PtL1–Pt(L6)<sub>2</sub> on HCT 116 cells after 48 h of treatment. The anticancer efficiency of all tested compounds is listed in **Table 2**. Results of the anti-proliferation test show that all tested compounds have a dose-dependent

effect. **Fig. 10** shows the photomicrographic images of cancer cells treated with these compounds for 48 h. First, cells treated with the standard drug 5-FU ( $IC_{50} = 7.3 \mu\text{M}$ ) show decreased viability. The cells reveal apoptotic characteristic features because cell membrane blebbing, crescent-shaped nuclei, and nuclear condensation can be observed in the treated cells. HCT 116 cells treated with PtL1 show a moderate cytotoxic effect ( $IC_{50} = 53.9 \mu\text{M}$ ). The treatment significantly reduces the doubling time of the cell population compared with the negative control. Treatment with PtL2 shows a moderate inhibitory effect on cell proliferation ( $IC_{50} = 61.3 \mu\text{M}$ ), and the affected morphology of the treated cells can be clearly visualized in the photomicrograph. The photomicrograph of HCT 116 cells treated with PtL3 shows the strong cytotoxic effect of the complex ( $IC_{50} = 2.8 \mu\text{M}$ ). PtL3 is found to affect the proliferation of almost all cells of the group and causes the cells to lose their spindle-shaped structure and adherent property. Thus, except for a few live cells, only cellular debris can be seen in the growth medium. The photomicrograph of HCT 116 cells treated with PtL4 show poor anti-proliferative activity ( $IC_{50} = 149.9 \mu\text{M}$ ). Treatment with PtL5 shows a considerable anti-proliferative effect ( $IC_{50} = 22 \mu\text{M}$ ) compared with the control. The photomicrograph shows that treatment of HCT 116 cells with PtL5 reduces cell proliferation and renders the cells less viable. Finally, treatment of HCT 116 cells with Pt(L6)<sub>2</sub> demonstrates significant anti-proliferative activity because the  $IC_{50}$  ( $7.8 \mu\text{M}$ ) is found to be more or less similar to that of the standard reference. The results presented in Table 2 revealed that as compared to the compounds PtL1, PtL2, PtL3, PtL5 and PtL6, which has no substituent in the isatin scaffold or substituent with methyl or fluoride, substitution of nitro group at its position-5 (PtL4;  $IC_{50} = 149 \mu\text{M}$ ) reduced its activity [49].

[Insert Fig. 9, Table 2, and Fig. 10]

### 3. Conclusion

Six novel square planar platinum(II) complexes, namely, PtL1 to Pt(L6)<sub>2</sub>, with a tridentate ligands were synthesized and characterized using elemental analysis and various spectroscopic techniques. The crystal structure of Pt(L6)<sub>2</sub> shows that it is a four-coordinate complex with a slightly distorted square-planar geometry. Results of binding studies showed that these complexes have been found to interact with CT DNA through an intercalative mode, which was supported by absorption studies, (the intrinsic binding constant ( $K_b$ ) values were found to be  $3.5 \times 10^4$  to  $3.29 \times 10^6 \text{ M}^{-1}$ ), fluorescence and viscosity measurement techniques, and their affinity to DNA follows the order Pt3 > PtL1 > PtL6 > PtL2 > PtL5 > PtL4, which can be attributed to the presence of an extended aromatic phenyl ring which allows an intercalating ligand to deeply penetrate into the DNA base pairs. Finally, results of *in vitro* anti-proliferative activity against HCT 116 cells showed dose-dependent cytotoxicity of the synthesized complexes, with significantly low IC<sub>50</sub> values ranging from 2.8  $\mu\text{M}$  to 149.9  $\mu\text{M}$ . The anti-proliferative effect of PtL3 was stronger than that of the standard 5-FU, whereas Pt(L6)<sub>2</sub>, PtL5, PtL1, and PtL2 showed significant anti-proliferation activity (less or equal to that of 5-FU). The strongest IC<sub>50</sub> value for PtL3 compared to other complexes may be attributed to the presence of fluorine atom at C5 in isatin moiety [50]. Therefore, the platinum(II) complexes of thiosemicarbazone Schiff bases with isatin moiety can be promising anti-neoplastic agents. The toxic potentials of the most active complexes and their anti-tumor efficacies are under investigation in animal models and will be reported in due course.

**Abbreviations**

CT DNA	Calf-thymus DNA
DMSO	Dimethyl sulfoxide
EB	Ethidium bromide
5-FU	5-fluorouracil
UV-Vis	UV-visible
ROS	Reactive oxygen species

**Acknowledgments**

The authors thank the Malaysian Government and Universiti Sains Malaysia for the FRGS research grant. AQA thanks the Ministry of Higher Education and the University of Sabha (Libya) for a scholarship.

**Appendixes Supplementary data**

Crystallographic data for the structural analysis of the complex  $\text{Pt}(\text{L6})_2$  has been deposited with the Cambridge Crystallographic Data Center, CCDC No. CCDC909984. Copies of this information may be obtained free of charge from The Director, CCDC, 12 Union Road, Cambridge, CB2 1EZ, UK (fax: +44 1233336 033; e-mail: deposit@ccdc.cam.ac.uk).

**References**

- [1] U. Olszewski, E. Ulsperger, K. Geissler, G. Hamilton, *J. Exper. Pharm.* 3 (2011) 43.
- [2] A. S. Abu-Surrah, M. Kettunen, *Curr. Med. Chem.*, 13 (2006) 1337.
- [3] K. -B. Huang, Z. -F. Chen, Y. -Ch. Liu, Z. -Q. Li, J. -H. Wei, M. Wang, X. -L. Xie, H. Liang, *Eur. J. Med. Chem.* 64 (2013) 554.
- [4] P. Kalyani, M. Adharvanachary, Prakash. M. M. S. Kinthada, *Int. J Pharm. Biomed. Sci.* 3(2) (2012) 70.
- [5] I. Kostova, *Recent Patents on Anti-Cancer Drug Dis.* 1(2006) 1.
- [6] A. -M. Florea, D. Büsselberg, *Cancers* 3 (2011) 1351.
- [7] N. Farrell, *Compreh. Coord. Chem. II* 9 (2003) 809.
- [8] C. Iysel, V. T. Yilmaz, A. Golcu, E. Ulukaya, O. Buyukgungor. *Bioorg. Med. Chem. Lett.*, 23 (2013) 2117.
- [9] A. I. Matesanz, C. Hernández, A. Rodríguez, P. Souza, *Dalton Trans.*, 40(2011) 5738.
- [10] N. Raman, S. Sobha, M. Selvaganapathy, *Int. J. Pharma & Bio Sci.* 3 (2012) 251.
- [11] A. Q. Ali, N. E. Eltayeb, S. G. Teoh, A. Salhin, H.-K. Fun, *Acta Cryst.* (2012). E68, o962.
- [12] A. Q. Ali, N. E. Eltayeb, S. G. Teoh, A. Salhin, H.-K. Fun, *Acta Cryst.* (2011). E67, o3476.
- [13] A. Q. Ali, N. E. Eltayeb, S. G. Teoh, A. Salhin, H.-K. Fun, *Acta Cryst.* (2012). E68, o285.
- [14] A. Q. Ali, N. E. Eltayeb, S. G. Teoh, A. Salhin, H.-K. Fun, *Acta Cryst.* (2012). E68, o953.
- [15] A. Q. Ali, N.E. Eltayeb, S. G. Teoh, A. Salhin, H.-K. Fun, *Acta Cryst.* (2012). E68, o955.

- [16] Bruker (2005). APEX2, SAINT and SADABS. Bruker AXS Inc., Madison, Wisconsin, USA.
- [17] Sheldrick, G. M. (2008). *Acta Cryst.* A64, 112.
- [18] N. Mahalakshmi, R.Rajavel, *Asian J. Bioch. Pharm. Res.* 2 (1) (2011) 525.
- [19] W. C. Chen, L. D. Wang, Y. T. Li, Z. Y. Wu, C. W. Yan, *Trans. Met. Chem.* 37 (2012) 569.
- [20] A. Hussain, S. Gadadhar, T. K. Goswami, A. A. Karande, A. R. Chakravarty *Eur. J. Med. Chem.* 50 (2012) 319.
- [21] M. N. Dehkordi, A. K. Bordbar, P. Lincoln, V. Mirkhani, *Spectrochimica Acta Part A* 90 (2012) 50.
- [22] H. Paul, T. Mukherjee, M.G.B. Drew, P. Chattopadhyay, *J. Coord. Chem.* 65(8) (2012) 1289.
- [23] Y. Li, Z. Y. Yang, M. F. Wang, *J. Fluoresc* 20 (2010) 891.
- [24] M. B. Ahamed, A. F. Aisha, Z. D. Nassar, J. M. Siddiqui, Z. Ismail, S. M. Omari, C. R. Parish, A. M. Majid, *Nut. Cancer* 64 (2012) 89.
- [25] L. M. Chen, J. Liu, J. C. Chen, C. P. Tan, S. Shi, K. C. Zheng, L. N. Ji, *J. Inorg. Bioch.* 102 (2008) 330.
- [26] I. Eryazici, C. N. Moorefield, G. R. Newkome, *Chem. Rev.* 108 (9) (2008) 1834.
- [27] R.V. Singh, N. Fahmi, M.K. Biyala, *J. Iran. Chem. Soci.*, 2 (1) (2005) 40.
- [28] G. Dehghan, M. Arvin, M. Hoseinpourfeizi, *Intern. Confe. on Med. Biolo. & Pharmace. Scie. (ICMBPS'2011) Pattaya Dec. (2011)* 499.
- [29] C. Y. Zhou, J. Zhao, Y. B. Wu, C. X. Yin, P. Yang, *J. Inorg. Bioch.* 101 (2007)10.
- [30] S. Rajalakshmi, T. Weyhermüller, A. J. Freddy, H. R. Vasanthi, B. U. Nair, *Eur. J. Med. Chem.* 46 (2011) 608.
- [31] R. Eshkourfu, B. Čobeljić, M. Vujčić, I. Turel, A. Pevec, K. Sepčić, M. Zec, Radulović, T.S. Radić, D.Mitić, K. Andjelković, D. Sladić, *J. Inorg. Bioc.* 105 (2011) 1196.

- [32] Ng. Lingthoingambi, N. Rajen Singh , M. Damayanti, J. Chem. Pharm. Res. 3(6) (2011) 187.
- [33] L. Leelavathy, S. Anbu, M. Kandaswamy, N. Karthikeyan, N. Mohan, Polyhedron 28 (2009) 903.
- [34] D. S. Raja, N. S.P. Bhuvanesh, K. Natarajan, Inorg. Chim. Acta 385 (2012) 81.
- [35] N. Shahabadi, S. Kashanian, A. Fatahi Bioi. Chem. Appl., Volume 2011, Article ID 687571 doi:10.1155/2011/687571
- [36] N. H. Khan, N. Pandya, N. Ch. Maity , M. Kumar, R. M. Patel, R. I. Kureshy, S. H.R. Abdi, S. Mishra, S. Das, H. C. Bajaj, Eur. J. Med. Chem. 46 (2011) 5074.
- [37] N. H. Khan, N. Pandya, M. Kumar, P.K. Bera, R. I. Kureshy, S. H. R. Abdi , H. C. Bajaj , Org. Biomol. Chem., 8 (2010) 4297.
- [38] K. C. Skyrianou, F. Perdih, A. N. Papadopoulos, I. Turel, D. P. Kessissoglou, G. Psomas J. Inorg. Biochem. 105 (2011) 1273.
- [39] N. Shahabadi, S. Kashanian, F. Darabi, Eur. J. Med. Chem. 45 (2010) 4239.
- [40] H. Pervez, N. Saira, M. S. Iqbal, M. Yaqub, K. M. Khan, Med. Chem. Res. 22 (2013) 5878.
- [41] B. Coban, U. Yildiz, A. Sengul. J. Biol. Inorg. Chem., 18 (2013) 461.
- [42] R. Palchaudhuri, P. J Hergenrother, Current Opinion in Biotechno. 18 (2007) 497.
- [43] M. Tarui, M. Doi, T. Ishida, M. Inoue, S. Nakaike , K. Kitamura, Biochem. J. 304 (1994) 271.
- [44] H. Guo, J. Lu, Z. Ruan, Y. Zhang, Y. Liu, L. Zang, J. Jiang, J. Huang, J. Coord. Chem. 65(2) (2012) 191.
- [45] L. B. Liao, H. Y. Zhou, X. M. Xiao, J. Molec. Struc. 749 (2005) 108.
- [46] N. Raman, S. Sobha, J. Serb. Chem. Soc. 75 (6) (2010) 773.
- [47] S. Kashanian, M. M.Khodaei, P. Pakravan, H. Adibi, Mol. Biol .Rep. 39 (2012) 3853.

- [48] F. Liu, K. Wang, G. Bai, Y. Zhang, L. Gao, *Inorg. Chem.* 43 (2004) 1799.
- [49] H. Pervez, N. Manzoor, M. Yaqub, A. Khan, K. M. Khan, F. Nasim, M. I. Choudhary, *Letters in Drug Design & Discovery*, 7 (2) (2010) 103.
- [50] K. L. Vine, L. Matesic, J.M. Locke, D. Skropeta, *Recent highlights in the development of isatin based anticancer agents*, Bentham Science Publishers, UAE, 2013.

ACCEPTED MANUSCRIPT

Scheme 1. Synthetic route and structures for compounds L1H-L6H.

Scheme 2. Synthetic route and structures for compounds PtL1-PtL6.

Fig.1. The structure of PtL6 complex, showing 50% probability displacement ellipsoids and atomic numbering.

Fig.2. The crystal packing of PtL6, viewed approximately along the *a* axis.

Fig.3. Absorption spectra of PtL3 in the absence and in the presence of increasing amounts of DNA in Tris HCl buffer (pH-7.2). [PtL3] = 50  $\mu$ M, [DNA] = 0-163.58  $\times 10^{-6}$  M. The arrow shows the effect of increasing of CT-DNA concentration on the absorption intensity.

Fig. 3a. Comparative plot of [DNA]/( $\epsilon_a - \epsilon_f$ ) vs. [DNA] for the absorption titration of CT-DNA with complex PtL3 in Tris HCl buffer (pH-7.2);  $K_p = 3.29 \times 10^6 \text{ M}^{-1}$  ( $R = 0.9721$ ,  $n = 6$  points).

Fig.4. Absorption spectra of PtL6 in the absence and in the presence of increasing amounts of DNA in Tris HCl buffer (pH-7.2). [PtL6] = 50  $\mu$ M, [DNA] = 0-163.58  $\times 10^{-6}$  M. The arrow shows the effect of increasing of CT-DNA concentration on the absorption intensity.

Fig. 4a. Comparative plot of [DNA]/( $\epsilon_a - \epsilon_f$ ) vs. [DNA] for the absorption titration of CT-DNA with complex PtL6 in Tris HCl buffer (pH-7.2);  $K_p = 3.6 \times 10^5 \text{ M}^{-1}$  ( $R = 0.9909$ ,  $n = 6$  points).

Fig.5. Emission spectra of PtL2 in the absence and in the presence of increasing amounts of DNA in Tris HCl buffer (pH-7.2). [PtL2] = 50  $\mu$ M, [DNA] = 0-163.58  $\times 10^{-6}$  M. The arrow shows the emission intensity increases upon increasing the CT-DNA concentration.

Fig.6. Emission spectra of PtL6 in the absence and in the presence of increasing amounts of DNA in Tris HCl buffer (pH-7.2). [PtL6] = 50  $\mu$ M, [DNA] = 0-163.58  $\times 10^{-6}$  M. The arrow shows the emission intensity increases upon increasing the CT-DNA concentration.

Fig.7. Effect of increasing amounts of PtL1 ( — ), PtL2 ( — ) and PtL3 ( — ) on the relative viscosity of CT-DNA at 37.0 ( $\pm 0.1$ )  $^{\circ}$ C.

Fig.8. Effect of increasing amounts of PtL4 ( ■ ), PtL5 ( ■ ) and PtL6 ( ■ ) on the relative viscosity of CT-DNA at 37.0 ( $\pm 0.1$ ) °C.

Fig.9. Effect of different concentrations of platinum(II) complexes of isatin thiosemicarbazones derivatives (PtL1-PtL6) on human colorectal cancer cells (HCT 116) after 48 hours treatment.

Fig.10. Picture of cancer cells treated with platinum(II) complexes of isatin thiosemicarbazones derivatives (PtL1-PtL6) for 48 hr.

ACCEPTED MANUSCRIPT



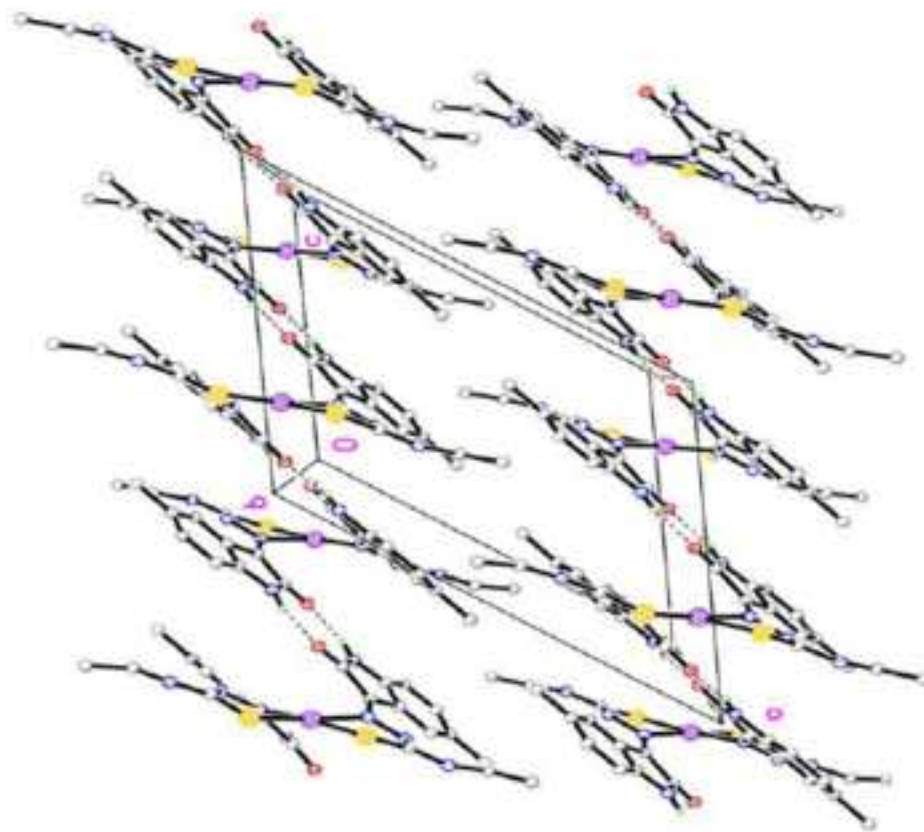


Figure 2

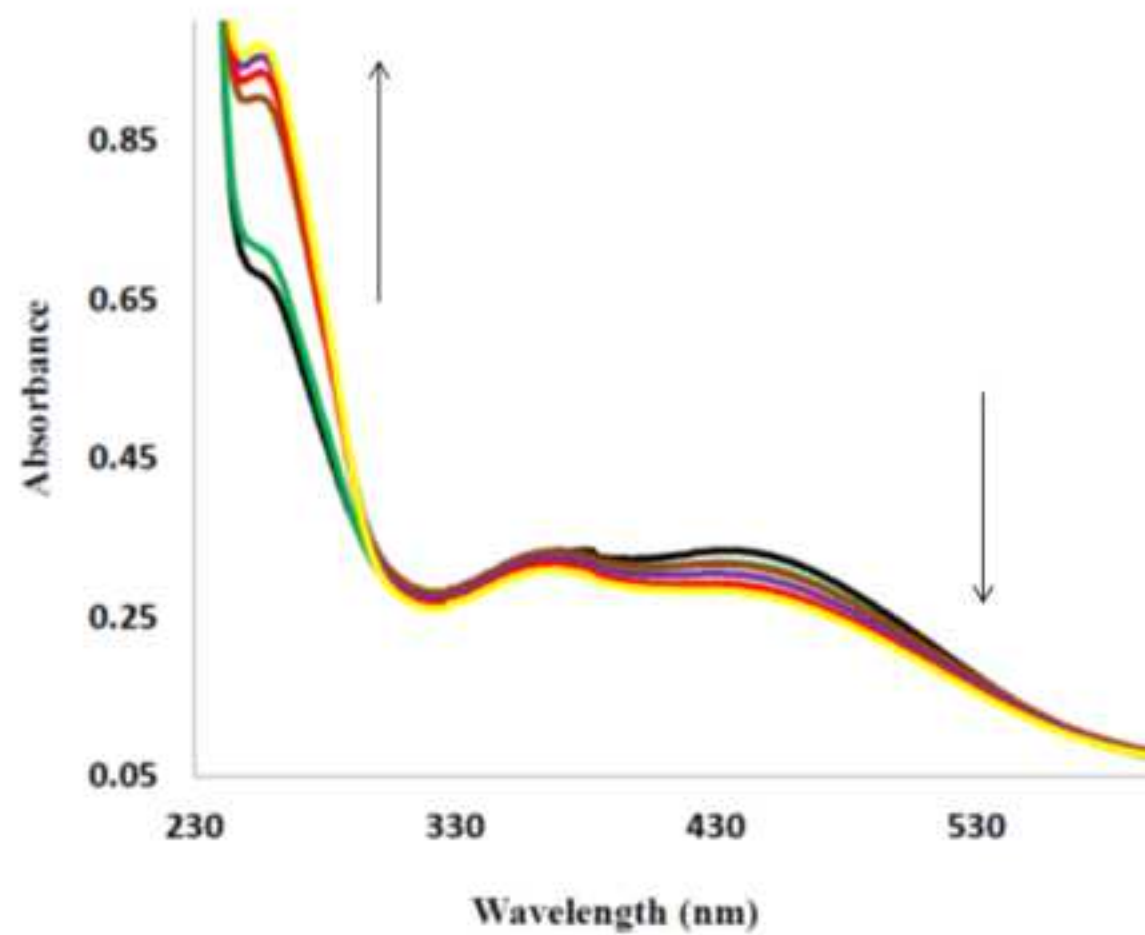


Figure 3

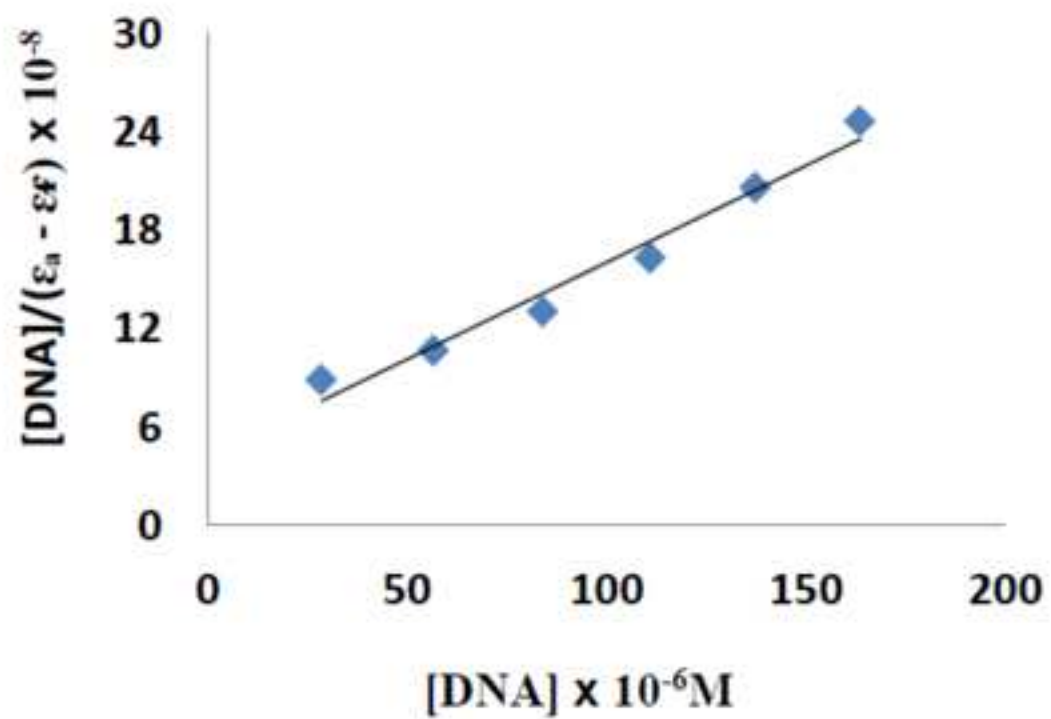


Figure 3a

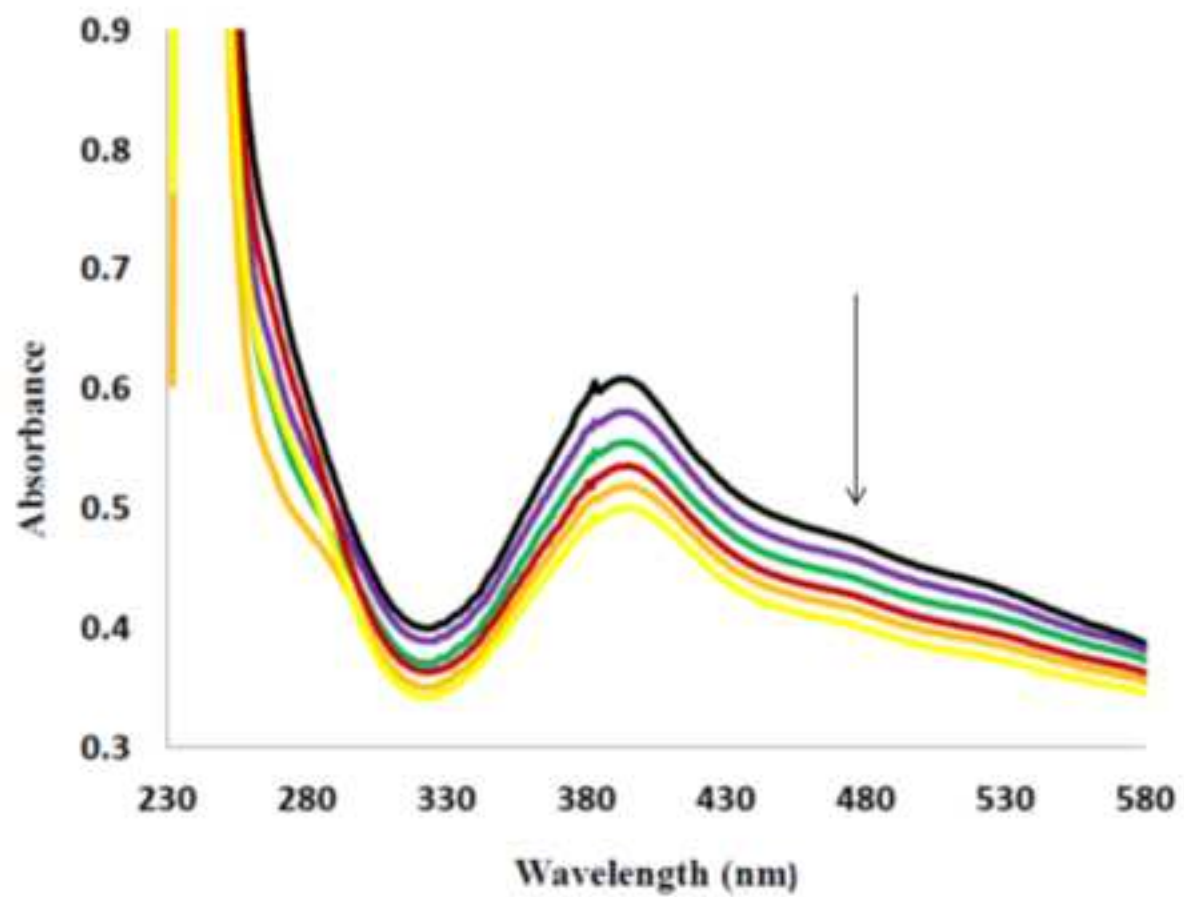


Figure 4

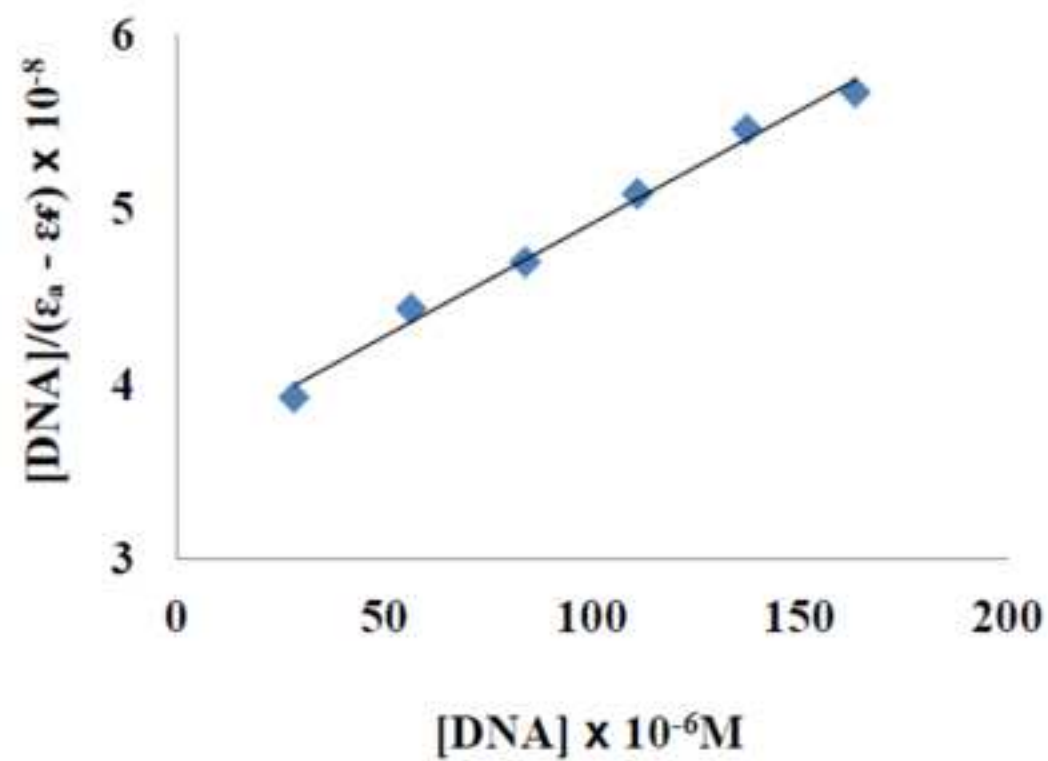


Figure 4a

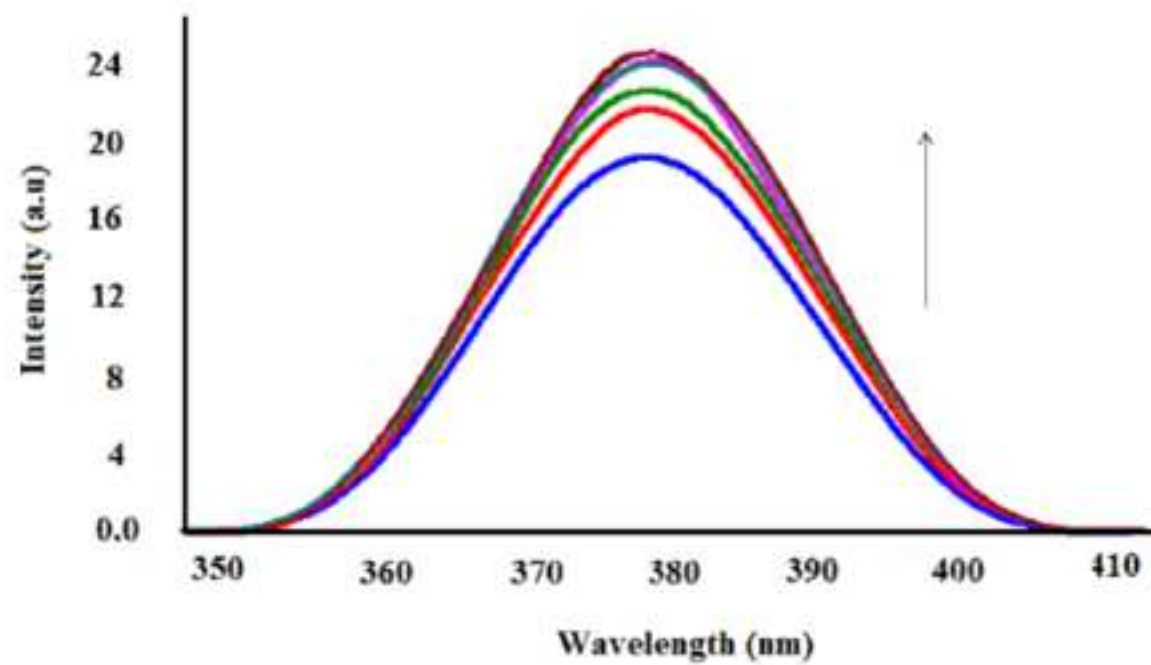


Figure 5

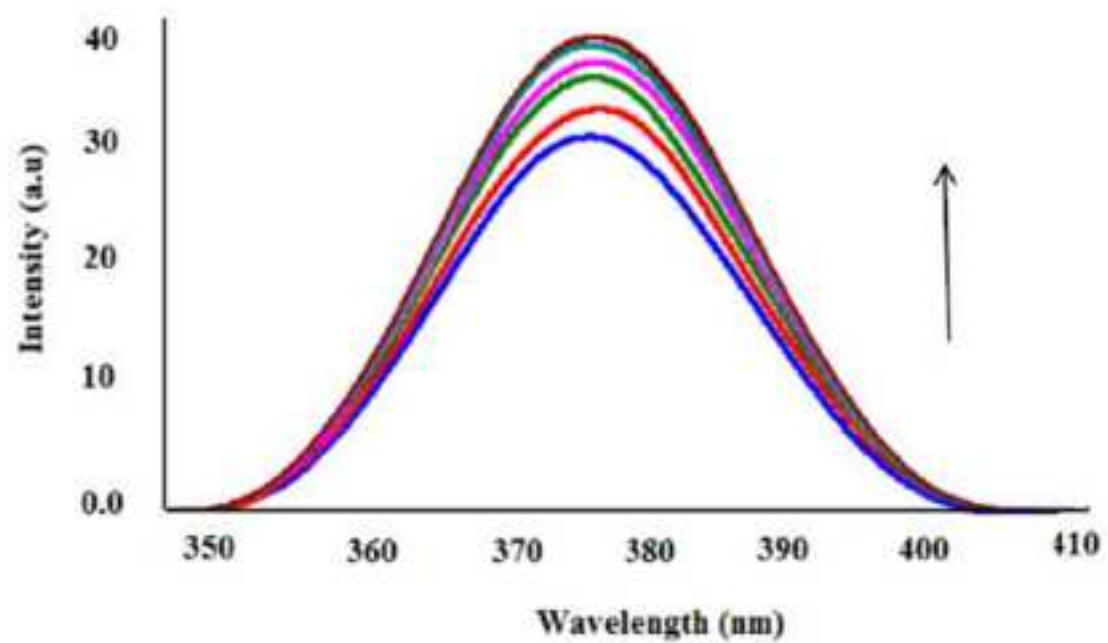


Figure 6

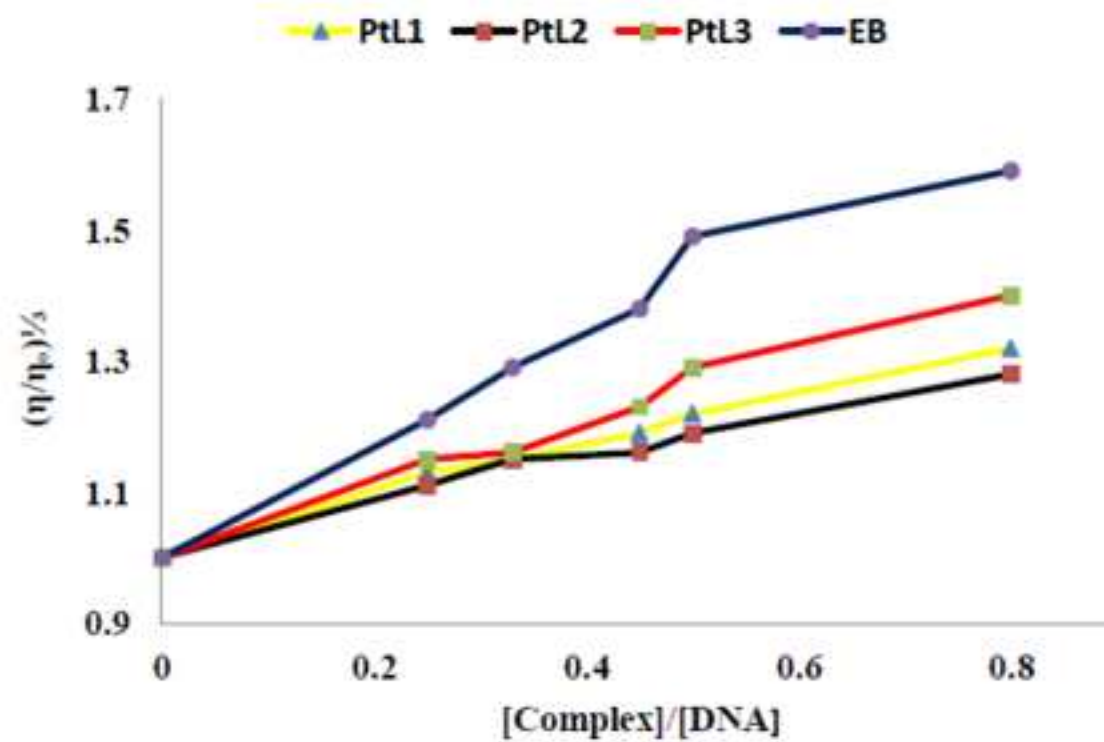


Figure 7

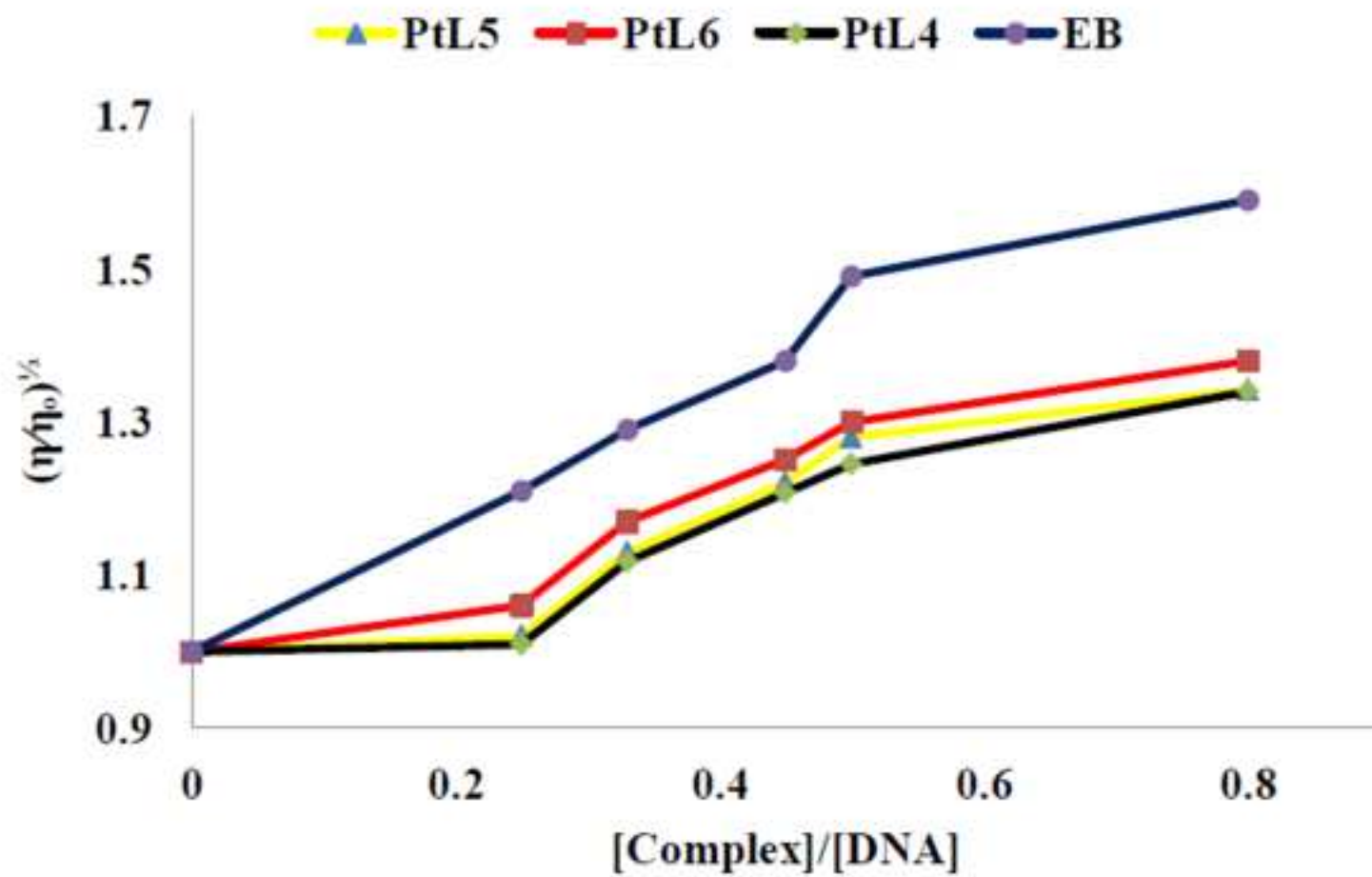


Figure 8

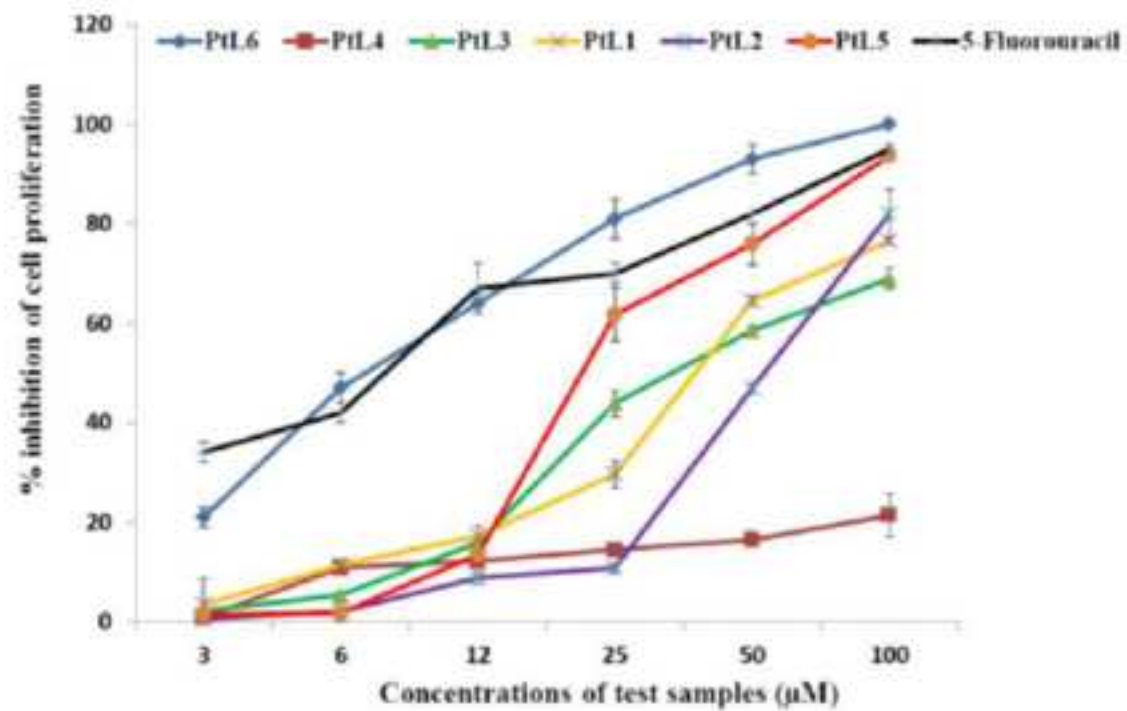


Figure 11

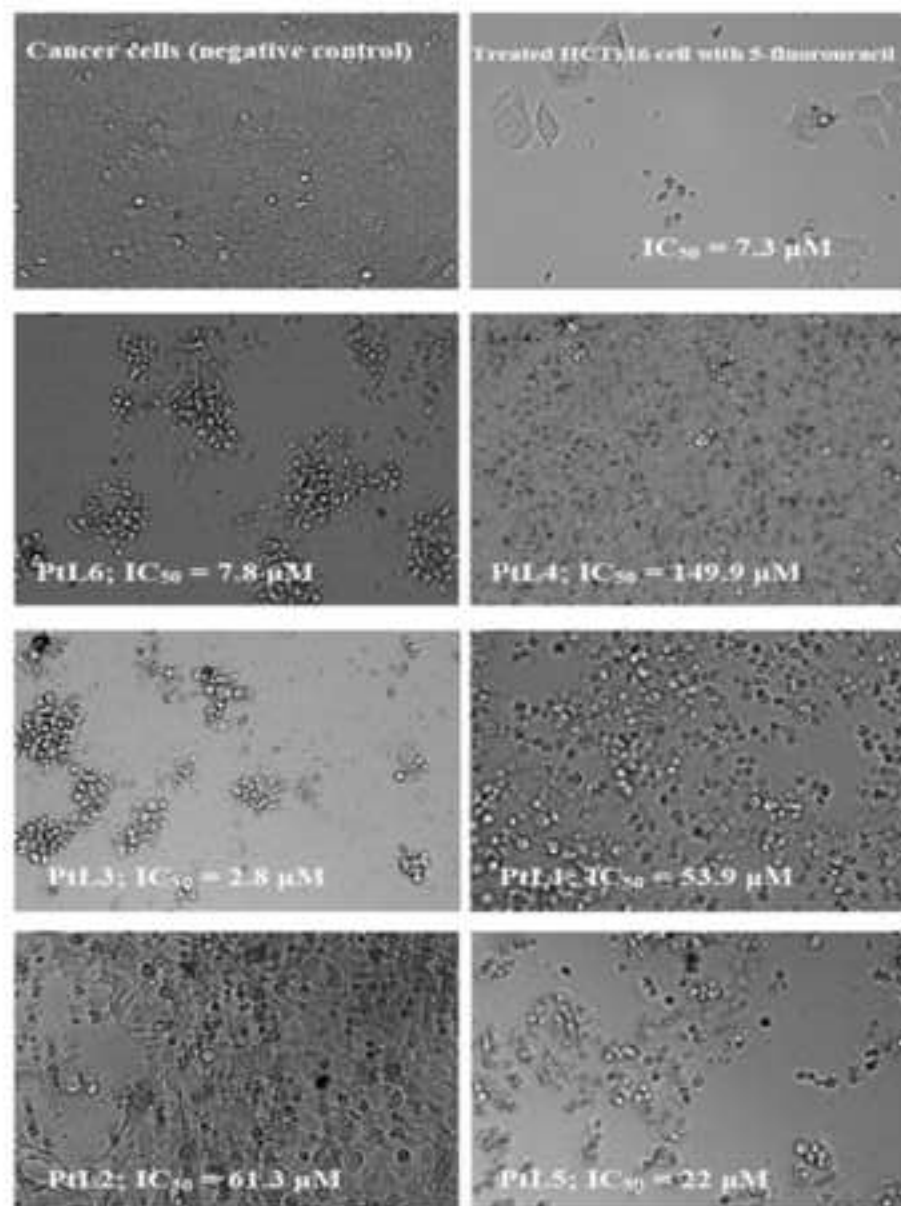
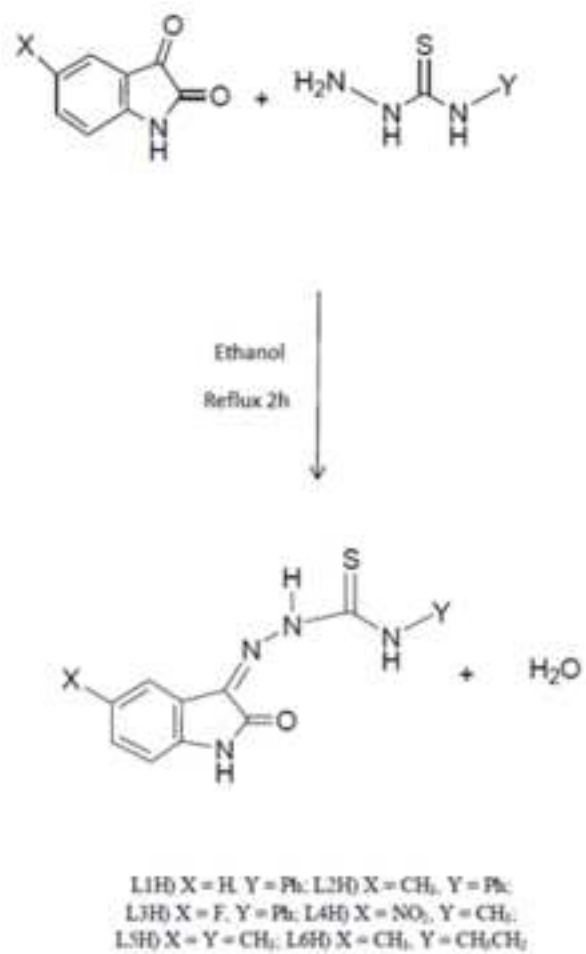
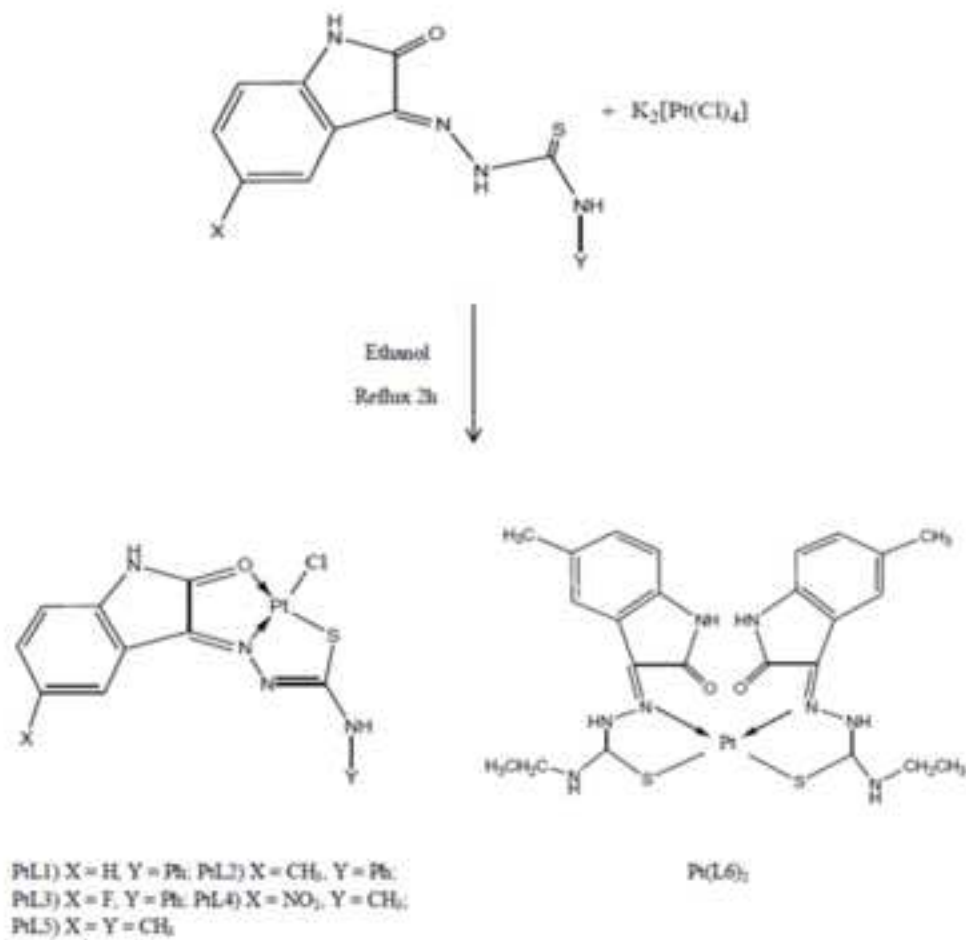


Figure 12



Scheme 1.



Scheme 2.

Table 1. Crystallographic data for complex PtL6.

Formula	C <sub>24</sub> H <sub>26</sub> N <sub>8</sub> O <sub>2</sub> Pt S <sub>2</sub>
<i>F</i> <sub>w</sub>	717.75
<i>T</i> (K)	100 (1)
Cryst syst	Monoclinic
Space group	C2/c
<i>a</i> (Å)	14.1172(2)
<i>b</i> (Å)	19.8743(4)
<i>c</i> (Å)	11.3475(2)
$\beta$ (°)	127.044(1)
<i>V</i> (nm <sup>3</sup> )	2541.19(8)
<i>Z</i>	4
D <sub>c</sub> (Mg m <sup>-3</sup> )	1.876
<i>F</i> (000)	1408
Cryst dimens (mm)	0.14 x 0.19 x 0.40
$\theta$ range (°)	2.0-35.4
<i>hkl</i> ranges	-22 < <i>h</i> < 23 -24 < <i>k</i> < 32 -18 < <i>l</i> < 18
Data/parameters	5705/178
Goodness-of-fit on <i>F</i> <sup>2</sup>	1.17
Final <i>R</i> indices [ <i>I</i> > 2 <i>s</i> ( <i>I</i> )]	<i>R</i> <sub>1</sub> = 0.0262 <i>wR</i> <sub>2</sub> = 0.0828
Highest peak/ deepest hole	$\Delta\rho_{\max} = 4.90\text{e } \text{Å}^{-3} / \Delta\rho_{\min} = -1.74\text{e } \text{Å}^{-3}$

**Table2. IC<sub>50</sub> Values of Pt(II) Complexes**

Compound	IC <sub>50</sub> value/ $\mu\text{M}$
PtL1	53.9
PtL2	61.3
PtL3	2.8
PtL4	149.9
PtL5	22.0
PtL6	7.8

**Synthesis of platinum(II) complexes of isatin thiosemicarbazones derivatives : *in vitro* anti-cancer  
and Deoxyribosenucleic Acid Binding Activities**

**Amna Qasem Ali <sup>a</sup>, Siang Guan Teoh <sup>a\*</sup>, Abdussalam Salhin <sup>a</sup>, Naser Eltahir Eltayeb <sup>b</sup>,**

**Mohamed B. Khadeer Ahamed <sup>c</sup> and AMS Abdul Majid <sup>c</sup>**

<sup>a</sup>School of Chemical Sciences, Universiti Sains Malaysia, Minden-11800, Pulau Pinang, Malaysia,

<sup>b</sup>Department of Chemistry, Sciences & Arts College – Rabigh, King AbdullAziz University , Rabigh ,  
Saudi Arabia,

<sup>c</sup>EMAN Research and Testing Laboratory, School of Pharmaceutical Sciences,

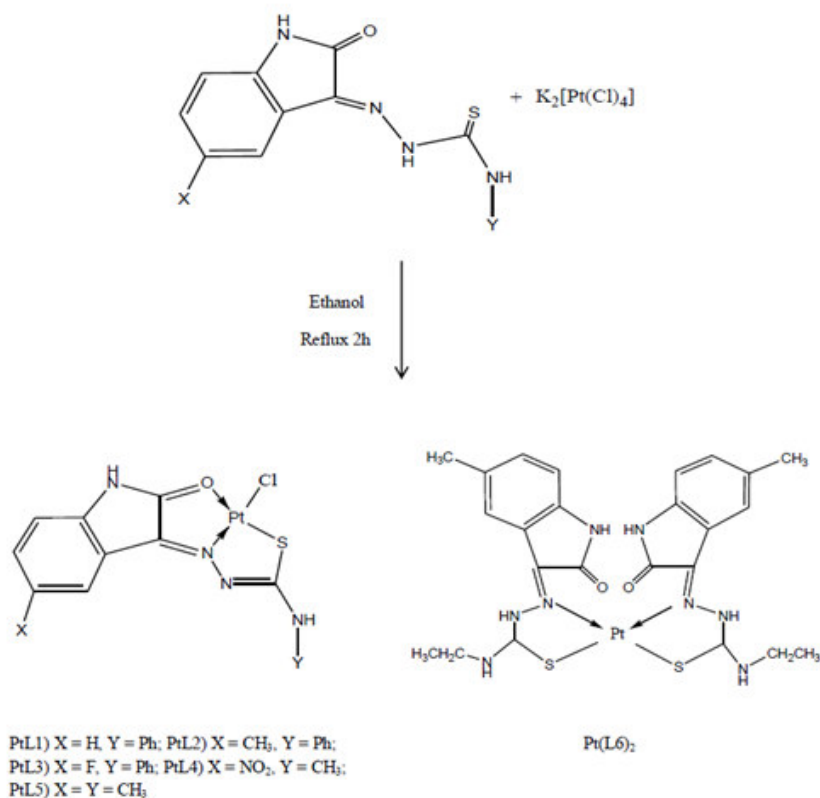
Universiti Sains Malaysia, 11800-Minden, Pulau Pinang, Malaysia

**Highlights**

☐ Six new platinum(II) complexes of thiosemicarbazone Schiff base with isatin moiety were synthesized.

☐ The interaction of these compounds with calf thymus (CT) DNA exhibited high intrinsic binding constant.

☐ The *in vitro* anti-proliferative study clearly establishes the anticancer potency of some of these complexes against (HCT 116).



New platinum (II) complexes with derivatives of thiosemicarbazone Schiff base with isatin moiety were synthesized. The interaction of these compounds with calf thymus (CT) DNA exhibited high intrinsic binding constant. **PtL1 –PtL6** showed ability to cleave the DNA by oxidative and hydrolytic pathway. The *in vitro* anti-proliferative study clearly establishes the anticancer potency of these complexes against HCT 116.